INTERNATIONAL JOURNAL FOR NUMERICAL METHODS IN FLUIDS, VOL. 1, 225–235 (1981)

APPLICABILITY OF ALGEBRAIC MODELS BASED ON UNIDIRECTIONAL FLOW TO DUCT FLOW WITH LATERAL MOTION

D. NAOT
Department of Nuclear Engineering, Technion, Haifa, Israel

AND

W. RODI
S.F.B. 80, University of Karlsruhe, Karlsruhe, West Germany

SUMMARY

The solution for the stress transport turbulence model equations for the situation where the flow is unidirectional is now commonly applied to flows with weak secondary currents in closed ducts, open channels, and rod bundles in nuclear reactor channels. Here, perturbations to the unidirectional flow solutions are studied by solving the exact equations using an iterative procedure. Now the equations also contain the small lateral velocity gradients formerly neglected. The applicability as well as the limitation of the use of the unidirectional flow turbulence model for the description of channel flow with lateral motion are discussed. Modifications for weak lateral motion are suggested.

KEY WORDS Turbulence Fluid Flow Mathematical Models Reynolds Stresses Channels Lateral Motion

1. INTRODUCTION

A direct outcome of the development of the stress transport turbulence models is the ability to predict correctly the fact that shear flows are associated with two substantially different normal stresses in the lateral plane. This achievement permitted the prediction of the secondary currents in various configurations of channel flows. For this purpose a solution was developed for the stress transport equations in local equilibrium conditions for the unidirectional flow where the flow, being in a single direction, has derivatives with respect to the two co-ordinates in the lateral plane perpendicular to the main flow.

This solution, also referred to as the algebraic stress model, was applied by Launder and Ying,[1] Tatchel,[2] Gessner and Emery,[3] Neti and Eichhorn[4] and others to the calculation of secondary currents in square duct flow; and by Gosman and Rapley,[5] Benodekar and Date,[6] Trupp and Aly[7] to the calculation of flow in non-circular domains including rod bundles in nuclear reactors. Recently, the authors applied the model to the prediction of secondary currents induced by the free surface in open channels (Rodi and Naot[8]). the use of the algebraic stress model is attractive as it is more simple with respect to full stress transport calculations (Naot *et al.*[9], and Reece[10]). It is therefore important to examine its limitations.

In the present work the limitations due to the fact that the lateral velocity gradients are not considered in the evaluation of the production of the turbulent stresses are discussed. It became apparent, also, that attempts to include in future calculations other sources of weak lateral motion such as thermal-gravity driven motion, lateral weak injections, channel

0271–2091/81/030225–11$01.10
 Received 24 February 1981

curvature driven currents, etc., will require modifications to the algebraic stress model based on the unidirectional flow.

The inclusion of the lateral mean velocity gradients in the calculation of the turbulent stress production is considered here as perturbation. Special reference is made to three aspects:

(i) estimation of perturbations typical for channel flow,
(ii) attempts to account for the perturbations
and
(iii) estimation of the overall effect in square ducts.

These are important steps for research groups developing computing algorithms for flows in engine passages, channels and rod bundles in nuclear reactors. The present work is associated with the work performed at the S.F.B. 80, University of Karlsruhe, in the context of mathematical modelling of turbulent flow in rivers and open channels.

2. THE UNIDIRECTIONAL FLOW ALGEBRAIC MODEL

Basically the algebraic stress models are derived from the stress transport turbulence model equations assuming a hypothetical condition of local equilibrium where the production of turbulence balances its dissipation. In that case the model equations defined by Naot *et al.*[9] and Launder *et al.*[11] transform to:

$$(1-\alpha)\pi_{ij}+\beta D_{ij}+\gamma\tfrac{4}{3}kE_{ij}+\tfrac{2}{3}(\alpha-\beta)\pi\delta_{ij}-\frac{\epsilon}{k}[\overline{u_iu_j}C_1+(1-C_1)\tfrac{2}{3}k\delta_{ij}]=0. \tag{1}$$

Here,

$$\pi_{ij}=-\left(\overline{u_iu_l}\frac{\partial\bar{U}_j}{\partial x_l}+\overline{u_ju_l}\frac{\partial\bar{U}_i}{\partial x_l}\right), \tag{2}$$

$$D_{ij}=-\left(\overline{u_iu_l}\frac{\partial\bar{U}_l}{\partial x_j}+\overline{u_ju_l}\frac{\partial\bar{U}_l}{\partial x_i}\right), \tag{3}$$

$$\tfrac{4}{3}kE_{ij}=\tfrac{4}{3}k\left(\frac{\partial\bar{U}_i}{\partial x_j}+\frac{\partial\bar{U}_j}{\partial x_i}\right), \tag{4}$$

k is the turbulence energy, ϵ is the energy dissipation rate and α, β, γ and C_1 are the model coefficients. Here $\pi=\frac{1}{2}\pi_{ll}$, and the energy $k=\frac{1}{2}\overline{u_iu_i}$. The numerical coefficients considered are the near wall set given in Reference 11, $\alpha=0{\cdot}704$, $\beta=-0{\cdot}169$, $\gamma=-0{\cdot}273$, $C_1=1{\cdot}0$.

The unidirectional case is the special situation where the flow has vanishing mean velocity gradients except for $\partial\bar{U}/\partial y$ and $\partial\bar{U}/\partial z$. In that case equation (1) transforms to

$$\frac{\epsilon}{k}C_1\overline{v^2}=\tfrac{2}{3}(\alpha+\tfrac{1}{2}\beta)\pi+\tfrac{2}{3}(C_1-1)\epsilon-\beta\left[\overline{uv}\frac{\partial\bar{U}}{\partial y}-\overline{uw}\frac{\partial\bar{U}}{\partial z}\right], \tag{5}$$

$$\frac{\epsilon}{k}C_1\overline{\omega^2}=\tfrac{2}{3}(\alpha+\tfrac{1}{2}\beta)\pi+\tfrac{2}{3}(C_1-1)\epsilon+\beta\left[\overline{uv}\frac{\partial\bar{U}}{\partial y}-\overline{uw}\frac{\partial\bar{U}}{\partial z}\right], \tag{6}$$

$$\frac{\epsilon}{k}C_1\overline{uv}=-[(1-\alpha)(\overline{v^2}+\overline{vw}\tan\psi)+\beta\overline{u^2}-\tfrac{2}{3}\gamma k]\frac{\partial\bar{U}}{\partial y}, \tag{7}$$

$$\frac{\epsilon}{k}C_1\overline{uw}=-[(1-\alpha)(\overline{\omega^2}+\overline{vw}\cot\psi)+\beta\overline{u^2}-\tfrac{2}{3}\gamma k]\frac{\partial\bar{U}}{\partial z}, \tag{8}$$

and

$$\frac{\epsilon}{k} C_1 \overline{vw} = -\beta\left(\overline{uv}\frac{\partial \bar{U}}{\partial z} + \overline{uw}\frac{\partial \bar{U}}{\partial y}\right). \tag{9}$$

Here

$$\psi = \text{arctg}\left(\frac{\partial \bar{U}}{\partial z}\Big/\frac{\partial \bar{U}}{\partial y}\right), \tag{10}$$

is the angle formed between the z-axis and the tangent to the streamwise velocity contours.

Equations (5)–(9) can be solved for the turbulent stresses. The solution given in terms of the mean velocity gradients, the turbulent energy, the energy dissipation rate, and the model coefficients is commonly referred to as the algebraic model. The algebraic steps, not shown here, were first given by Launder and Ying.[1] Recently Naot[12] showed that the solution can be simply derived from the shear flow solution by merely rotating the co-ordinates.

An interesting feature of the algebraic model is the observation that the two main shear stresses, $\overline{uv}$ and $\overline{uw}$, can be calculated using the same eddy viscosity μ_t

$$\overline{uv} = -\mu_t \frac{\partial \bar{U}}{\partial y} \tag{11}$$

and

$$\overline{uw} = -\mu_t \frac{\partial \bar{U}}{\partial z}, \tag{12}$$

with

$$u_t = C_\mu k^2/\epsilon, \tag{13}$$

and

$$C_\mu = \tfrac{2}{3}[(1-\alpha)(\alpha+2\beta+C_1-1)+\beta(3-2\alpha-\beta+C_1-1)-\gamma C_1]\frac{1}{C_1^2}.$$

This analytic result stemming from equations (5)–(9), simplifies considerably the numerical calculations of the streamwise mean velocity as it permits the use of methods based on scalar eddy viscosity, such as the Spalding–Patankar[13] algorithm.

Another important feature of the algebraic model is the observation that the stresses which control the secondary currents can be calculated directly from the main streamwise velocity gradients $\partial \bar{U}/\partial y$ and $\partial \bar{U}/\partial z$:

$$\overline{v^2} = \tfrac{2}{3}k(\alpha+\tfrac{1}{2}\beta+C_1-1)\frac{1}{C_1} + \frac{\beta k}{C_1 \epsilon}\mu_t\left[\left(\frac{\partial \bar{U}}{\partial y}\right)^2 - \left(\frac{\partial \bar{U}}{\partial z}\right)^2\right], \tag{14}$$

$$\overline{w^2} = \tfrac{2}{3}k(\alpha+\tfrac{1}{2}\beta+C_1-1)\frac{1}{C_1} - \frac{\beta k}{C_1 \epsilon}\mu_t\left[\left(\frac{\partial \bar{U}}{\partial y}\right)^2 - \left(\frac{\partial \bar{U}}{\partial z}\right)^2\right], \tag{15}$$

and

$$\overline{vw} = \frac{2\beta k}{C_1 \epsilon}\mu_t\left(\frac{\partial \bar{U}}{\partial y}\right)\left(\frac{\partial \bar{U}}{\partial z}\right). \tag{16}$$

This is a major simplification in the numerical simulation of secondary currents[3–7] as we may

use equations (14), (15) and (16) to prepare and store the motivating sources of the lateral momentum equations before solving these equations.

The advantages of the algebraic model are therefore apparent. Still, the algebraic model is based on the unidirectional flow which is an idealization of channel flow and may lead to errors. The objective of the present work is to estimate the errors made by not accounting for the lateral mean velocity gradients typical of channel flows, in the calculation of the production of the stresses. To this end an iterative procedure for the solution of the full stress transport model equations in the conditions of local equilibrium was developed.

3. AN ITERATIVE PROCEDURE

The algorithm is based on successive substitutions of an approximate solution into the full stress balance equation given in the form:

$$\begin{aligned}\overline{u_i u_j}^{(n+1)} = \frac{k^{(n)}}{C_1 \epsilon^{(n)}} \Bigg\{ & \gamma_3^2 k^{(n)} \left(\frac{\partial \bar{U}_i}{\partial x_j} + \frac{\partial \bar{U}_j}{\partial x_i} \right) \\ & + (\alpha - 1) \left(\overline{u_i u_l}^{(n)} \frac{\partial \bar{U}_j}{\partial x_l} + \overline{u_j u_l}^{(n)} \frac{\partial \bar{U}_i}{\partial x_l} \right) \\ & - \beta \left(\overline{u_i u_l}^{(n)} \frac{\partial \bar{U}_l}{\partial x_j} + \overline{u_j u_l}^{(n)} \frac{\partial \bar{U}_l}{\partial x_i} \right) \\ & + \tfrac{2}{3} \left[(\beta - \alpha) \overline{u_m u_l}^{(n)} \frac{\partial \bar{U}_m}{\partial x_l} + (C_1 - 1) \epsilon \right] \delta_{ij} \Bigg\} \end{aligned} \tag{17}$$

Here, the upper index (n) denotes the iteration counter. At each iteration new values for $\overline{u_i u_j}$ are obtained by substituting the values calculated at the former iteration in the right-hand side of equation (9). In addition, to satisfy the condition of local equilibrium the dissipation ϵ was adjusted at each iteration and was set equal to the production π. The procedure was found stable as is shown for the case of shear flow in Figure 1. Still, to accelerate convergence the new stresses were under-relaxed to 50 per cent. The results, also shown in Figure 1, emphasize the role of the under-relaxation as a practical means of reducing the number of iterations.

Apparently the procedure is very simple and its application for the numerical evaluation of the turbulent stresses is straightforward. Unfortunately, this is not necessarily

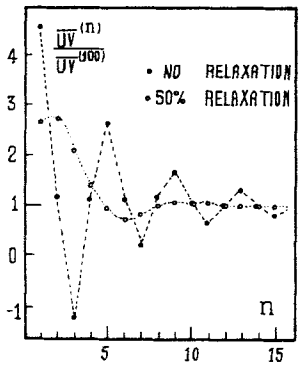

Figure 1. Convergency of shear stress $\overline{uv}$ in Shear Flow ($\psi = 0$)

so if one wishes to use the new iterative procedure to adjust continuously the algebraic model in numerical calculations of developing three-dimensional channel flows. In that case the procedure should be used in the innermost loop. Since the innermost loop is performed for each grid node and is iterated a few times for each streamwise step,[13] a substantial increase in computing time is expected. Therefore, the authors decided not to apply the procedure for that purpose at the present time. Instead, typical perturbations were studied on the basis of 100-iteration runs and simple corrections to the algebraic model were suggested.

4. SMALL PERTURBATIONS

Three types of small derivatives were added to the basic unidirectional flow in order to examine the influence of the lateral velocity gradients. The perturbation imposed consisted of

$$(I)\ \frac{\partial \bar{W}}{\partial y}, \qquad (II)\ \frac{\partial \bar{V}}{\partial z} \quad \text{and} \quad (III)\ \frac{\partial \bar{W}}{\partial z} = -\frac{\partial \bar{V}}{\partial y}, \tag{18}$$

representing lateral shear, (I) and (II), as well as lateral strain (III). For weak perturbations it is plausible to assume linearity of the effects. We therefore assume that the three perturbations represent all other possibilities for which estimations can be obtained simply by a superposition rule. The three perturbations imposed are defined by:

$$\delta_1 = \frac{\partial \bar{W}}{\partial y}\left[\left(\frac{\partial \bar{U}}{\partial y}\right)^2 + \left(\frac{\partial \bar{U}}{\partial z}\right)^2\right]^{-1/2}, \qquad 0 < \delta_1 < 0{\cdot}1, \tag{19}$$

$$\delta_2 = \frac{\partial \bar{V}}{\partial z}\left[\left(\frac{\partial \bar{U}}{\partial y}\right)^2 + \left(\frac{\partial \bar{U}}{\partial z}\right)^2\right]^{-1/2}, \qquad 0 < \delta_2 < 0{\cdot}1, \tag{20}$$

and

$$\delta_3 = \frac{\partial \bar{W}}{\partial z}\left[\left(\frac{\partial \bar{U}}{\partial y}\right)^2 + \left(\frac{\partial \bar{U}}{\partial z}\right)^2\right]^{-1/2}, \qquad 0 < \delta_3 < 0{\cdot}1. \tag{21}$$

Assuming the maximum of the lateral gradient of the streamwise velocity $\bar{U}$ to be in the y-direction, the angle ψ was restricted to $0 < \psi < 45°$ for practical reasons.

The results are given in Figures 2–7. Obviously, the solutions for $\delta = 0$ represent the unidirectional solutions. Observing the results we should note that $\delta = 0{\cdot}05$ and $\delta = 0{\cdot}10$ are relatively high with respect to the values which characterize the lateral motion in straight closed ducts and open channels. Such values however, may be reached in curved channels and in the case of lateral injection into channel flow.

Generally the deviations from the unidirectional flow solutions show two types of effects: (a) The influence of the lateral velocity gradients on the main stresses $\overline{uv}$ and $\overline{uw}$, as shown in Figure 3, 5 and 7; (b) The influence of the lateral velocity gradients on the stresses which control the secondary currents $\overline{w^2}$, $\overline{v^2}$ and $\overline{vw}$, as shown in Figures 2, 4 and 6.

The complete understanding of the results is not simple, as we base our intuition on the concept of scalar eddy viscosity. Indeed, equation (17) implies that as far as previous iterations result in non-vanishing trace $2k = \overline{u_i u_i}$, an additional iteration will contain among other terms:

$$\overline{u_i u_j}^* = -\frac{1}{\sigma}\mu_t\left(\frac{\partial \bar{U}_i}{\partial x_j} + \frac{\partial \bar{U}_j}{\partial x_i}\right), \tag{22}$$

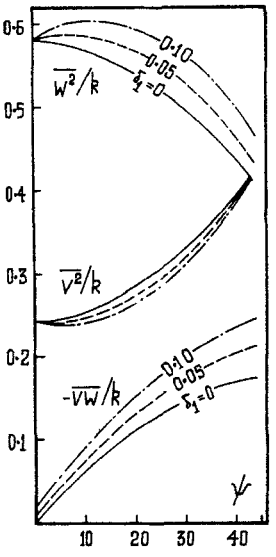

Figure 2. Stresses controlling lateral motion subjected to lateral shear I

with

$$\sigma = \tfrac{3}{2}C_\mu C_1/(1-\alpha+\beta-\gamma). \tag{23}$$

Unfortunately equation (22) provides an explanation only for the deviations of the second type as will be shown in Section 5.

In Figures 3 and 5 the influence of the lateral shear expressed by δ_1 and δ_2 on the main stress $\overline{uv}$ is shown. For example, with δ_1 and δ_2 smaller than 0·05 we do not expect deviations in $\overline{uv}$ greater than 10 per cent. The influence of the lateral shear on $\overline{uw}$ is somewhat more pronounced. Still, we should recall that this stress is of less importance in the calculation of the streamwise mean velocity. The most pronounced deviations from the unidirectional solution are due to the lateral strain as shown in Figure 7. Now, we find deviations greater than 10 per cent already for δ_3 greater than 0·02. Following the example

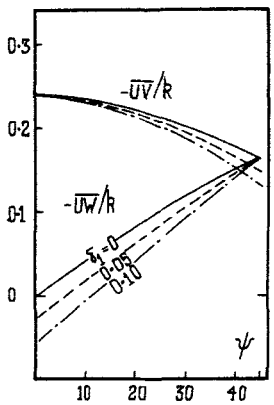

Figure 3. The main shear stresses $\overline{uv}$ and $\overline{uw}$ subjected to lateral shear I

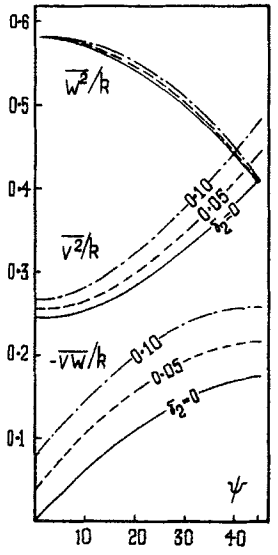

Figure 4. Stresses controlling lateral motion subjected to lateral shear II

and defining an acceptable percentage error, one may derive from Figures 3, 5 and 7 the upper bounds for δ_1, δ_2 and δ_3 which still permit use of equations (11) and (12) for the calculation of $\overline{uv}$ and $\overline{uw}$, respectively.

The influence of the lateral shear expressed by δ_1 and δ_2 on the normal stresses $\overline{v^2}$ and $\overline{w^2}$ is shown in Figure 2 and 4. Since deviations greater than 10 per cent are associated only with δ_1 and δ_2 greater than 0·08, we conclude that these stresses are practically unaffected by the presence of lateral shear. The deviations, due to the lateral strain shown in Figure 6, are more pronounced. Now deviations greater than 10 per cent in both $\overline{v^2}$ and $\overline{w^2}$ are found already for δ_3 greater than 0·02. The lateral stress $\overline{vw}$ is practically unaffected by the lateral strain as shown in Figure 6. This is not the case when lateral shear is considered as shown in Figure 2 and 4. Since the unidirectional solution for $\overline{vw}$ vanishes for small ψ, the relative error made by using equation (16) for $\overline{vw}$ may reach a high percentage no matter how small δ_1 and δ_2 are. Since the region of small ψ is very important, as discussed in Section 6, a simple approximation for these trends is needed and is now given.

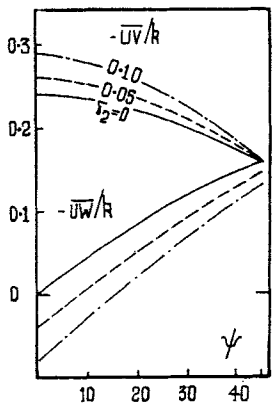

Figure 5. The main shear stresses $\overline{uv}$ and $\overline{uw}$ subjected to lateral shear II

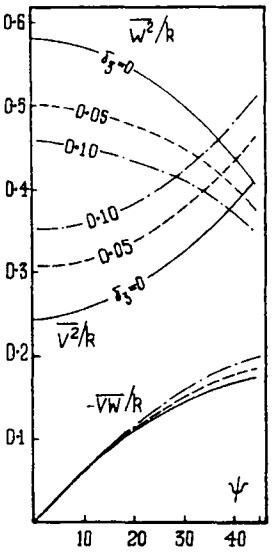

Figure 6. Stresses controlling lateral motion subjected to lateral strain

5. SIMPLE APPROXIMATION

To describe the deviations from the unidirectional flow solutions of the second type we suggest:

$$\overline{vw}_{\mathrm{DEV}} = -\mu_t \left(\frac{1}{\sigma_1} \frac{\partial \bar{W}}{\partial y} + \frac{1}{\sigma_2} \frac{\partial \bar{V}}{\partial z} \right), \tag{24}$$

$$\overline{v^2}_{\mathrm{DEV}} = -\mu_t \frac{2}{\sigma_3} \frac{\partial \bar{V}}{\partial y}, \tag{25}$$

$$\overline{v^2}_{\mathrm{DEV}} = -\mu_t \frac{2}{\sigma_3} \frac{\partial \bar{W}}{\partial z}. \tag{26}$$

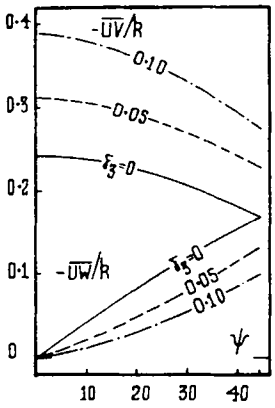

Fig. 7. The main shear stresses $\overline{uv}$ and $\overline{uw}$ subjected to lateral strain

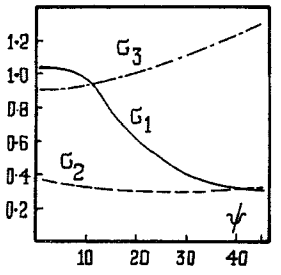

Figure 8. The turbulent Prandtl numbers

Here σ_1, σ_2 and σ_3 are parameters with a physical interpretation of turbulent Prandtl numbers.

In Figures 2 and 4 deviations of the lateral shear stress $\overline{vw}$ from the unidirectional flow solution ($\delta = 0$) are given. It was found possible to calculate these deviations using equation (24) and the values of σ_1 and σ_2, given in Figure 8. In Figure 6 deviations of the lateral normal stresses $\overline{v^2}$ and $\overline{w^2}$ from the unidirectional solution ($\delta = 0$) are given. The values of σ_3 needed in order that equations (25) and (26) describe these deviations are also shown in Figure 8. The importance of the approximation for the description of secondary currents in channels is now discussed.

6. STRAIGHT CHANNEL FLOW

First, we should show that the deviations from the unidirectional flow solutions are of importance and should not be neglected in the calculation of channel flow with weak lateral motion. To this end calculated[8,9] secondary currents in square duct flow were examined, and it was found that the three δ's are usually smaller than 0·01. Only those very close to the corner may reach values of about 0·03. Thus, apparently we should not be bothered by these perturbations.

Still, near the walls the situation is different. Here, ψ vanishes and is less than 6° for almost 90 per cent of the channel walls. In that case the errors made in describing $\overline{vw}$ by means of equation (16) may become large. For example, $\delta_2 = 0{\cdot}03$ and $\psi = 6°$ results in 50 per cent errors in $\overline{vw}$. Since the lateral stress $\overline{vw}$ is the main agent via which the lateral motion is damped by the wall, the overall prediction of the secondary currents may show large errors.

To examine this, equations (24), (25) and (26) with $\sigma_1 = \sigma_2 = \sigma_3 = 1$ were added to the unidirectional solution and were applied to the calculation of square duct flow. the results showed a reduction of 50 per cent in the lateral velocity adjacent to the walls, thus proving the importance of the deviations from the unidirectional flow solution.

7. CONCLUDING REMARKS

The overall accuracy of numerical simulation of channel flow with lateral motion depends on many factors including the model coefficients, wall proximity functions, etc. The present work was aimed at isolating the effects of neglecting the lateral velocity gradients in the calculation of the turbulent stress production.

It is recommended that the simple approximations given in Section 5 be used even if the lateral motion is weak. It seems that correcting $\overline{vw}$, $\overline{v^2}$ and $\overline{w^2}$ is sufficient as far as

$$[\bar{V}^2 + \bar{W}^2]^{1/2}/\bar{U} < 0{\cdot}05.$$

However, with stronger lateral motion the authors feel that simple approximations such as are given here may be an over-simplification and that a more complete model will be needed. In that case it will be necessary to correct all the turbulent stresses, including the main stresses $\overline{uv}$ and $\overline{uw}$.

APPENDIX: LIST OF SYMBOLS

C_1	Free redistribution model coefficient
C_μ	Eddy viscosity coefficient
D_{ij}	Part of the forced redistribution model
E_{ij}	Mean rate of train
k	Turbulence energy
n	Iteration index
u_i, u, v, w	Velocity fluctuations
$\bar{U}_i$	Mean velocity
$\bar{U}$	Streamwise mean velocity
$\bar{V}, \bar{W}$	Lateral mean velocity
x	Streamwise co-ordinate
y, z	Lateral co-ordinates

Greek symbols

α, β, γ	Forced redistribution model coefficients
δ_{ij}	Kronecker delta
$\delta_1, \delta_2, \delta_3$	Small perturbations
ϵ	Turbulent energy dissipation
μ_t	Turbulent eddy viscosity
π	Turbulent energy production
π_{ij}	Turbulent stresses production
$\sigma_1, \sigma_2, \sigma_3$	Turbulent Prandtl numbers
ψ	Isovel inclination angle

REFERENCES

1. B. E. Launder and W. M. Ying, 'Prediction of flow and heat transfer in ducts of square cross section', *Proc. Inst. Mech. Engrs*, **187**, 37/73, 455–461 (1973).
2. D. G. Tatchell, 'Convection processes in confined three dimensional boundary layers', *Ph.D Thesis*, Imperial College, London, 1975.
3. F. B. Gessner and A. F. Emery, 'A length scale model for developing turbulent flow in a square duct', in *Turbulent Boundary Layers* (Ed. H. E. Weber) ASME, New York, 1979.
5. A. D. Gosman and C. W. Rapley, 'A prediction method for fully developed flow through non-circular passages', in *Numerical Methods in Laminar & Turbulent Flows* (Ed. Taylor *et al.*), Pentech Press, London, 1978.
6. R. W. Benodekar and W. Date, 'Prediction of turbulent flow in finite rod clusters', *2nd Symp. Turbulent Shear Flows*, Imperial College, London (1979).
7. A. C. Trupp and A. M. M. Aly, 'Predicted secondary flows in triangular rod bundles', *Trans. ASME, J. Fluid Engrs*, **101**, 354–363 (1979).
8. W. Rodi and D. Naot, 'Numerical simulation of secondary currents in open channel flow with algebraic stress turbulence mode', *SFB 80 Report/T/187*, Karlsruhe, F.R.G. (1981).
9. D. Naot, A. Shavit and M. Wolfshtein, 'Numerical calculation of Reynolds stresses in a square duct with secondary flow', *Wärme and Stoffübertragung*, **7**, 151–161 (1974).
10. G. J. Reece, 'A generalized Reynolds stress model of turbulence', *Ph.D. Thesis*, Imperial College, London, 1976.

11. B. E. Launder, G. J. Reece and W. Rodi, 'Progress in the development of a Reynolds stress turbulence closure', *J. Fluid Mech.*, **68,** 537–566 (1975).
12. D. Naot, 'Two dimensional unidirectional turbulent flow in a local equilibrium', *Phys. Fluids*, **18,** 1813–1814 (1975).
13. S. V. Patankar and D. B. Spalding, 'A calculation procedure for heat mass and momentum transfer in three dimensional parabolic flows', *Int. J. Heat and Mass Transfer*, **15,** 1787–1806 (1972).